The Journal of Physiology

The neuromechanical adaptations to Achilles tendinosis

Yu-Jen Chang and Kornelia Kulig

Division of Biokinesiology and Physical Therapy, University of Southern California, Los Angeles, CA, USA

Key points

- Achilles tendinosis is a localized degenerative musculoskeletal disorder that develops over a long period of time and leads to a compliant human Achilles tendon.
- We demonstrate that the compliant Achilles tendon elicited a series of adaptations from different levels of the human movement control system, such as the muscle–tendon interaction, CNS control and other muscles in the lower leg.
- These results illustrate the human body's capacity to adapt to tendon pathology and provide the physiological basis for intervention or prevention strategies.

Abstract   Human movement is initiated, controlled and executed in a hierarchical system including the nervous system, muscle and tendon. If a component in the loop loses its integrity, the entire system has to adapt to that deficiency. Achilles tendon, when degenerated, exhibits lower stiffness. This local mechanical deficit may be compensated for by an alteration of motor commands from the CNS. These modulations in motor commands from the CNS may lead to altered activation of the agonist, synergist and antagonist muscles. The present study aimed to investigate the effect of tendon degeneration on its mechanical properties, the neuro-mechanical behaviour of the surrounding musculature and the existence of the CNS modulation accompanying tendinosis. We hypothesize that the degenerated tendon will lead to diminished tissue mechanical properties and protective muscle activation patterns, as well as an up-regulated descending drive from the CNS. Strong evidence, as reported in the present study, indicates that tendinotic tendons are more compliant compared to healthy tendons. This unilateral involvement affected the neuromuscular control on the involved side but not the non-involved side. The muscle–tendon unit on the tendinotic side exhibits a lowered temporal efficiency, which leads to altered CNS control. The altered CNS control is then expressed as an adapted muscle activation pattern in the lower leg. Taken together, the findings of the present study illustrate the co-ordinated multi-level adaptations to a mechanical lesion in a tendon caused by pathology.

Introduction

Successful human movement relies on the integrity of all the components involved in the hierarchical control system. This hierarchical system includes the CNS, the muscles and the tendons. The CNS plans, initiates and sends the motor command to the muscle (Wolpert *et al.* 2013). The muscle executes the motor command and generates force to pull on the tendon. The tendon modulates muscle force and controls the movement of a bone. Components that are lower in the hierarchical

system send feedback signals to assist the CNS in planning (Scott, 2004; Wolpert *et al.* 2013). If a single component in this loop loses its integrity, the entire system has to adapt to that deficiency (Loeb *et al.* 1999; Scott, 2004). This adaptation is possible only through a tight connection between sensory and motor systems (Fig. 1).

In vivo studies indicate reduced mechanical properties in tendinopathic human weight-bearing tendons (Arya & Kulig, 2010; Child *et al.* 2010; Kongsgaard *et al.* 2010). When the tendon is degenerated (i.e. the -opathy becomes an -osis), the human Achilles tendon exhibits higher strain and lower stiffness compared to that of tendons in healthy individuals (Arya & Kulig, 2010; Child *et al.* 2010). Among other factors, these reduced mechanical properties are attributed to disorganized collagen bundle architecture, thinner collagen fibres and increased water content in the extracellular matrix (Wang, 2006).

Reduced tendon mechanical properties lead to a less efficient muscle–tendon unit. Force generated by the muscle has to be transmitted to the bone through tendon efficiently. The electromechanical delay (EMD) is the time lag between the muscle activation and the mechanical force produced, which dictates the temporal efficiency of the muscle–tendon unit. Stiffness of the muscle–tendon unit was reported to increase and the EMD to shorten after training (Grosset, Piscione, Lambertz, & Perot, 2009). By contrast, a prolonged EMD was observed when the tendon is slackened by positioning the foot in plantar flexion (Muraoka *et al.* 2004). These studies suggest that EMD is negatively correlated with stiffness of the muscle–tendon unit. A similar relationship would be expected in Achilles tendinosis, consequently prolonging the time required for the transmission of force from muscle to bone.

Conceivably, the CNS readily adapts to the impaired temporal efficiency of the muscle–tendon unit. The adaptations may occur at spinal and supraspinal levels. Several factors can be attributed to alteration of the evoked spinal and supraspinal responses, including (1) altered neural drive in the descending corticospinal pathway; (2) altered motoneuron excitability; and (3) altered pre-synaptic inhibition (Aagaard *et al.* 2002; Upton, McComas, & Sica, 1971). It is well established that exercise training increases the spinal and supraspinal responses. This was observed as an increased H-reflex and V-wave after a 7 week and 14 week exercise training programme (Duclay & Martin, 2005; Aagaard *et al.* 2002). These studies suggest that the increase in motor neuron excitability after training is attributable to increased descending neural drive at the supraspinal level. This stimulus on motor neuron excitability may also be observed in people with Achilles tendinosis. The muscle is unintentionally 'trained' in the presence of a compliant tendon.

During functional activity, a protective mechanism prevents the already degenerated tendon from further injury or even rupture. It has been observed that experimental Achilles tendon pain induced by saline injection into the tendon can cause reduced EMG activity in agonist, antagonist and synergist muscles (Henriksen *et al.* 2011). Under this mechanism, the agonist and antagonist activity may be decreased to diminish the stress acting on the degenerated tendon. However, if the mechanical properties of the Achilles tendon are already reduced as a result of degeneration, the synergist activity may be increased to compensate for the mechanical deficiency accompanying tendinosis (Gardiner *et al.* 1986; Valero-Cuevas, 2005).

Taken together, the overall aim of the present study was to investigate the effect of tendon degeneration on its mechanical characteristics, the CNS modulation accompanying tendinosis and the neuromechanical behaviour of the surrounding musculature. We hypothesize that, in the presence of tendinosis, Achilles tendon mechanical properties will be reduced and motor neuron excitability will be enhanced. The amplitude of gastrocnemius' electrical activity will be decreased and accompanied by an increased contribution from other plantar flexors. Furthermore, the electrical activity of the gastrocnemius will occur earlier, signifying a modified feedforward control.

Methods

Subjects

Nineteen individuals aged 27–57 years (mean ± SD, 47 ± 7 years) participated in the present study. Among the nineteen individuals, nine were in the Achilles tendinosis (Tendinotic) group, who had (1) a history (i.e. at least one episode lasting more than 2 weeks) of unilateral Achilles discomfort in the Achilles tendon area; (2) an absence of pain in the Achilles tendon during walking or running at the time of participating in the study; and (3) a sonographically confirmed mid-substance (2–6 cm above the calcaneus) Achilles tendinosis, such as focal thickening and hypoechocity, specifically the anterior–posterior thickness of the thickest part of the tendinotic tendon was at least 2 mm thicker than the thickness measured at the same location on the opposite leg. The other 10 subjects served as control (Healthy) group. Individuals were excluded from this study if they had (1) a history of any prior major injury, or surgery involving the lower extremity and (2) diabetes, rheumatoid arthritis, systemic lupus erythromatosis, neurological disorders or any systemic disorders affecting the functioning of the lower extremity. Subjects' demographic and anthropometric data are provided in Table 1.

The procedures were approved by the Health Sciences Review Board at the University of Southern California. All subjects provided their written informed consent prior to participating in the present study. The study was conducted in accordance with the Declaration of Helsinki.

Table 1. Demographic and anthropometric data

	Tendinotic (*n* = 9)	Healthy (*n* = 10)
Age (years)	46.8 ± 6.3	48.7 ± 4.4
Body weight (kg)	74.1 ± 13.4	84.9 ± 19.7
Body height (m)	1.7 ± 0.08	1.7 ± 0.05
VISA-A	79.4 ± 22*	99.5 ± 1.2
GPAQ (MET-min)	4720 ± 3437.1	3983.3 ± 3080.0

Data are presented as the mean ± SD. MET, metabolic equivalent of task. *$P < 0.05$.

Victorian Institute of Sport Assessment – Achilles questionnaire (VISA-A) and Global Physical Activity Questionnaire (GPAQ)

Before the experiment, two questionnaires were administered for each subject:the GPAQ and the VISA-A. The GPAQ is a questionnaire comprising 16 questions developed by World Health Organization to provide information on physical activity participation (Armstrong & Bull, 2006). The VISA-A is an eight question questionnaire focusing on the severity of Achilles tendinopathy (Robinson *et al.* 2001). These two questionnaires were used to compare the differences in physical activity and severity of Achilles tendinopathy between the tendinotic and healthy groups.

Ultrasound imaging

Bilateral Achilles tendons of all subjects in the present study were imaged sonographically. Subjects were asked to lie prone on the test table with their feet hanging over the edge of the table. The posterior and superior tip of the calcaneus was identified by palpation, confirmed by imaging and marked on the skin. Longitudinal and transverse ultrasound images were taken for bilateral Achilles tendons on the mid-portion using grey-scale imaging mode (Sonoline Antares, Siemens Medical Solutions USA, Inc., Malvern, PA, USA; VFX 13–5 linear transducer). All images were screened for indicators of tendon degeneration (i.e. focal thickening, increases in cross-sectional area and areas of hypoechocity within the tendon).

Tendon mechanical measurement

Tendon mechanical properties were tested in accordance with the procedures reported in literature (Kubo *et al.* 2002; Maganaris & Paul, 2002; Arya & Kulig, 2010). Because slight modifications were implemented in the present study, a detailed description is provided. Subjects were lying prone on the HUMAC Norm isokinetic

dynamometer (CSMi Inc., Stoughton, MA, USA) with their testing foot tightly strapped on the foot plate. The axis of the dynamometer was aligned with the medial malleolus of the testing ankle. The ultrasound transducer was placed at the medial gastrocnemius muscle–tendon junction and stabilized by a custom-made transducer holder clamp. Reflective marker cluster was attached to the ultrasound transducer, whereas single markers were affixed to the distal attachment of the Achilles tendon on the calcaneus, medial and lateral condyle of the femur, and medial and lateral malleoli, to track the displacement of the ultrasound transducer and the distal attachment of the Achilles tendon. The experiment set-up is illustrated in Fig. 2

Surface EMG electrodes were attached bilaterally to the muscle belly of tibialis anterior (TA), gastrocnemius medial head (MG), soleus (SOL) and peroneal longus (PL) after the skin was prepared by rubbing with alcohol. Self-adhesive bipolar Ag/AgCl electrodes with 22 mm inter-electrode distance were used. The wireless sensor, which also served as the reference electrode, was taped to the skin right next to the surface electrodes. Electrical signals were transmitted through the sensor wirelessly to a TeleMyo 2400T receiver (Noraxon USA Inc., Scottsdale, AZ, USA). The preamplifiers have a double-differential input design, CMRR >100 dB, base gain at 400, input impedance >100 MΩohms and a first-order, high-pass filter at 10 Hz.

The subject was then asked to perform a maximal voluntary isometric plantar flexion contraction (MVIC) on the dynamometer to serve as the target torque. Followed by the MVIC, there were three ramped maximal voluntary isometric plantar flexion contractions, each with 5 s ramp-up, 2 s hold at maximal and 5 s ramp-down. A 2 min rest period was given between each contraction to ensure minimal impact from fatigue. A monitor displaying the torque output of the dynamometer was placed in front of the subject. The subjects were asked to control the cursors on the screen by plantar flexing their ankle to match the pre-determined torque curve. The position data of the reflective markers were captured using a 3-D motion analysis system (Qualisys AB, Gothenburg, Sweden) with three cameras at a sampling frequency of 150 Hz. The torque was recorded in synchronous with the positions of the reflective markers and the EMG signal by the motion analysis system (Qualisys AB) at a sampling frequency of 1500 Hz. Series ultrasound images took during the contractions were synchronized with the torque signal from the dynamometer and recorded at 30 frames s^{-1} with custom tailored LabVIEW software (National Instruments, Austin, TX, USA).

The moment arm of each Achilles tendon was estimated using the tendon travel method described by Maganaris & Paul (2002). The subjects remained in a prone position with their feet hanging freely over the table. The ankle joint

was slowly moved passively from 5 deg of dorsiflexion to 5 deg of plantar flexion. The excursion of the distal attachment of the Achilles tendon on the calcaneus during the passive movement was recorded using the motion capture system.

To calculate the tendon force, first, the torque that may potentially be contributed from the co-contraction of the tibialis anterior (TA) muscle was determined. For this, the EMG and torque during a ramped maximal isometric dorsiflexion contraction were recorded. The relationship between the TA EMG and the concurrent torque produced by the TA was then determined using a linear fit. The TA torque during isometric plantar flexion, calculated from the EMG amplitude, was added to the plantar flexor torque. After accounting for the torque from the TA, the equation applied was:
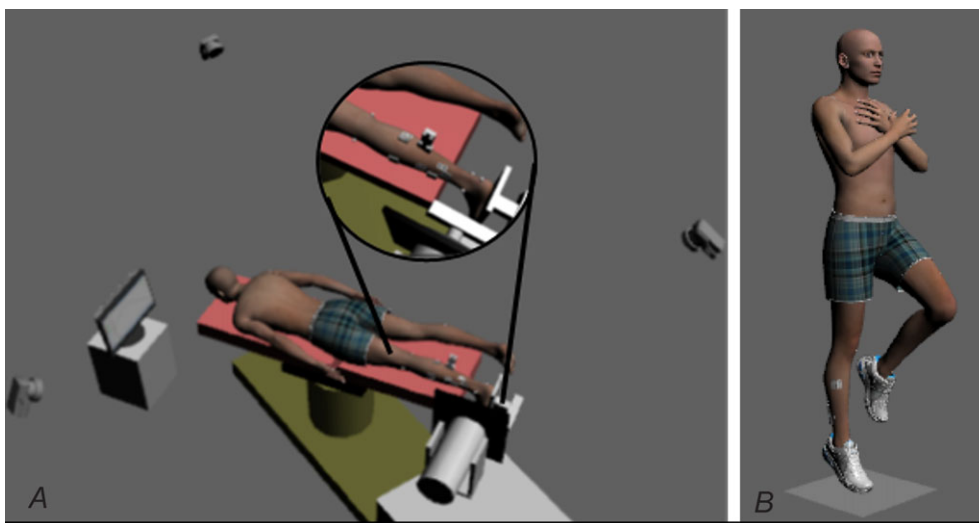
$$ATF = TQ/MA$$

where *ATF* denotes Achilles tendon force, *TQ* is the torque after accounting for TA torque and *MA* is the moment arm calculated as described above.
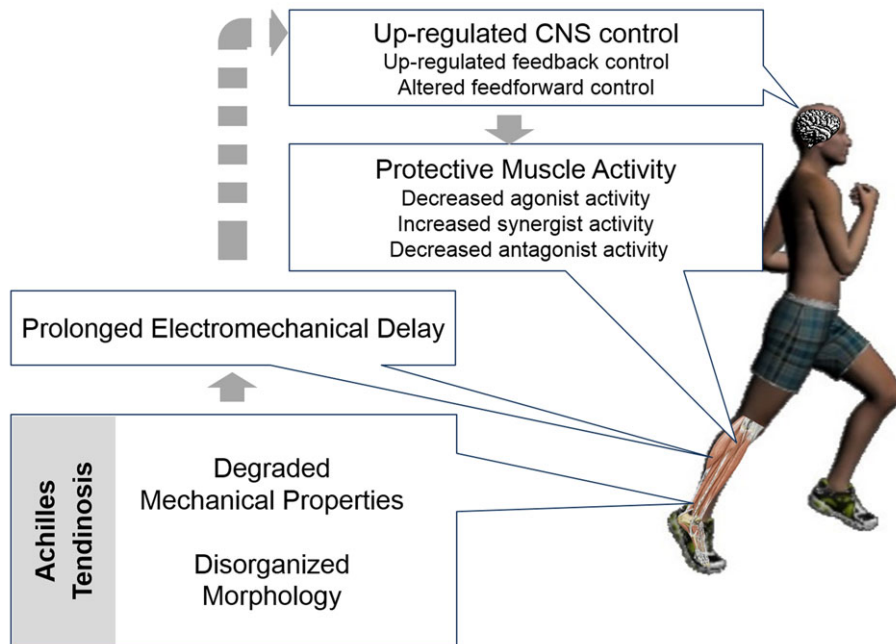
Figure 1. Conceptual framework
Effects of Achilles tendinosis on its mechanical properties, muscle–tendon interaction and CNS modulation

Figure 2. Experimental set-up
A, subjects' position for dynamometry, EMD and CNS adaptations. *B*, single leg hopping task.

The elongation of the tendon was calculated as a composite result from kinematics captured by the motion capture system, and the aponeurosis displacement from the serial ultrasound images. The displacement of the distal attachment of the Achilles tendon was manifested as heel marker displacement. The displacement of the aponeurosis was a combination of (1) aponeurosis displacement measured on the ultrasound images and (2) the displacement (and inclination) of the ultrasound transducer calculated from the motion capture system. The co-ordinates of the superficial distal point of the ultrasound image were determined for each frame by calculating from the position of the marker cluster on the ultrasound transducer. The distance between this superficial distal corner of the image and the heel marker was calculated from the kinematics. The distance of the aponeurosis to the superficial distal corner of the image was measured by tracking the speckles using ImageJ software with ManualTracking plug-in (US National Institutes of Health, Bethesda, Maryland, USA) (Fig. 3). The total tendon length was then calculated as the summation of the distance between the heel marker to the superficial distal point of ultrasound image and this point on the image to the distal aponeurosis. The overall tendon elongation was determined as the summation of the displacements from kinematics and aponeurosis movement.

The stiffness of the tendon during isometric contraction was determined by plotting the tendon force against tendon elongation. The stiffness was defined as the slope of the later 40% of the curve, which is the linear region of the curve (Arya & Kulig, 2010) (Fig. 4).

Measurement of EMD

The EMD was tested using an approach similar to that reported previously (Cavanagh & Komi, 1979; Muraoka *et al.* 2004; Esposito *et al.* 2011). The subjects were lying prone on the dynamometer, as described earlier, with their testing foot tightly strapped to the foot plate. Electrodes of an electrical stimulator were affixed to the subject's lower limb. The cathode electrode (diameter 15 mm) was taped over the tibial nerve at the back of the knee joint, and the anode electrode was placed on the anterior shin. A pulse with biphasic square wave with 250 μs phase duration was applied on the tibial nerve through the active electrode. The electric current was set at an intensity inducing visible muscle twitch. Evoked muscle activity on the EMG and the corresponding torque generated were recorded via the Qualisys system for further analysis to determine the EMD.

The electrically evoked muscle activity and the corresponding torque generated were used to determine the EMD of the muscle–tendon unit. The onset of the EMG and torque were determined when the amplitude of individual signals was 3 SDs greater than the baseline amplitude and lasted for 20 ms. The EMD was then defined as the temporal distance between the onset of muscle activity and the torque production (ms).

Spinal and supraspinal responses

The methods used to test the spinal and supraspinal responses follow those reported previously (Aagaard *et al.* 2002; Wang *et al.* 2011). To elicit spinal and supraspinal responses (H-reflex and V-wave), the placement
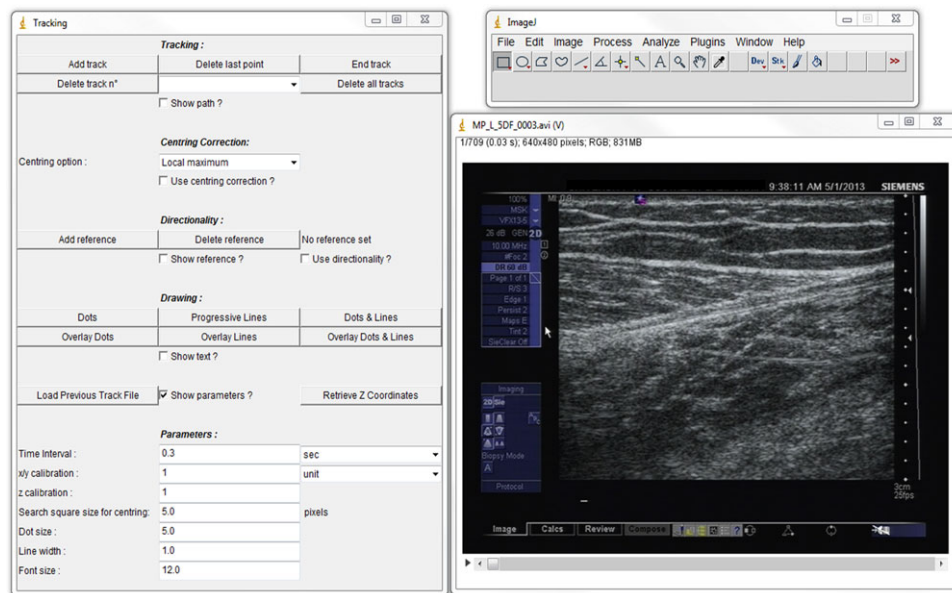
Figure 3. Tracking of the deep aponeurosis
Tracking was performed using ImageJ software with the manual tracking plug-in.

of cathode and anode electrodes was the same as that described above for measuring the EMD. Biphasic square wave pulses with 250 μs phase duration were applied on the tibial nerve through the active electrode, and the intensity was manually and gradually increased from 1 mA, with an interval of 10 s between stimulations, until a maximal H-reflex (H_{max}) was observed. The amplitude of the stimulation was recorded. The electrical stimulations were kept increasing until the maximal M-wave (M_{max}) was observed.

After testing the H-reflex, the subjects were asked to rest for 10 min, followed by electrical stimulations applied at the tibial nerve in the middle of maximal voluntary isometric plantar flexion contraction. MVIC was held for 5 s with a 2 min rest between trials. Electrical stimulations, with 150% of the amplitude to induce H_{max} at rest, were applied ~2 s after the contraction starts. With this stimulation, the V-wave was recorded.

The H-reflex and V-wave were normalized to maximal M-wave (H_{max}/M_{max} and V/M_{max}).

Preactivation and relative muscle activation

After the H-reflex and V-wave tests, subjects were asked to perform a unilateral rhythmic hopping task on a force platform. The same task was performed on both legs. Kinematic data during the hopping task were collected using a 3-D motion analysis system (Qualisys AB) at

a sampling frequency of 250 Hz with eight cameras. Simultaneous force platform data were collected from one AMTI force plate (Model #ORB-6-1; AMTI Corp., Newton, MA, USA) at a sampling frequency of 1500 Hz. Dynamic trials were captured when the subjects were asked to perform 20 single-legged hops on the AMTl force plate. Subjects were asked to hop 20 times at 2.2 Hz set by a metronome, with their arms crossed in front of the chest. This rate was chosen so that it was faster than self-selected hopping rate (~2 Hz) to emphasize the contribution from the ankle joint. Track Manager software (Qualisys AB) was used to digitize and record the kinetic and kinematic data.

The onset of the ground reaction force acquired from the force platform was determined when the value of the vertical ground reaction force exceeded 20 N during single-legged hopping. The onset of EMG activity of the medial gastrocnemius muscle was determined when the amplitude was 3 SD greater than the baseline amplitude. The preactivation (ms) was then calculated as the temporal distance between the onsets of the ground reaction force and the EMG.

The contribution index (CI) is defined as:

$$CI = \frac{\int MG + \int SOL}{\int MG + \int SOL + \int PL}$$

where each integration symbol represents the integrated EMG of the corresponding muscle. A ratio of 1 indicates no contribution from the peroneal longus muscle, whereas
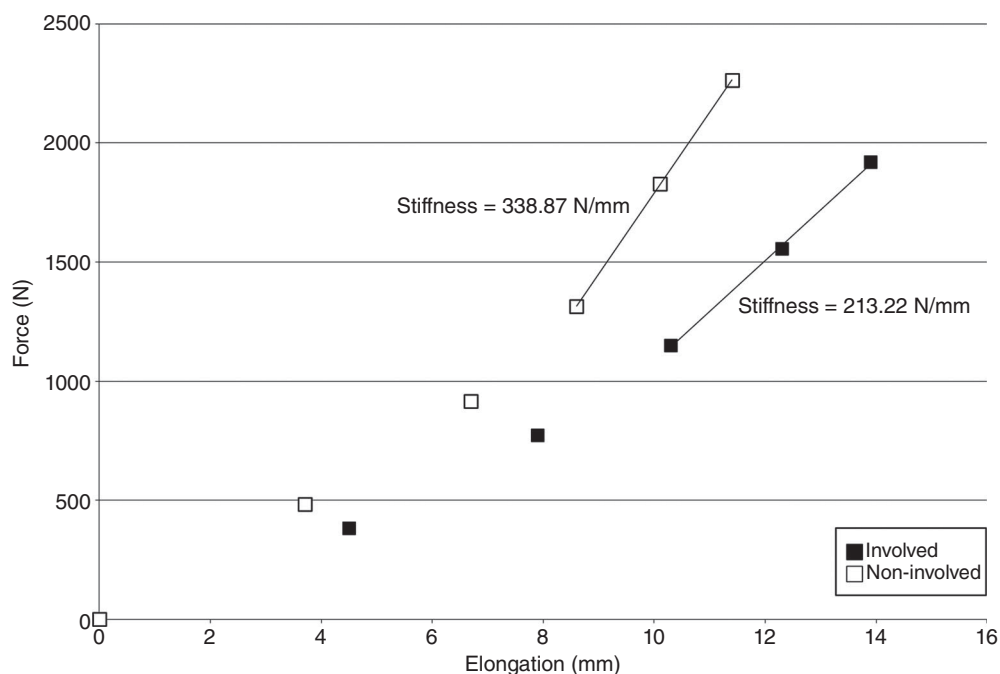
Figure 4. Representative force–elongation plot
Plot from a single tendinotic subject's involved (■) and non-involved (□) sides. The data are plotted at 0%, 20%, 40%, 60%, 80% and 100% of maximal Achilles tendon force for each side. The continuous line in each dataset is where the stiffness (slope) is calculated (60–100% of maximal Achilles tendon force).

a ratio of 0 suggests no contribution from the medial gastrocnemius or soleus muscle.

The co-contraction ratio (CCR) was calculated as the ratio of the ankle dorsiflexor (TA) to the summation of ankle plantar flexors (MG, SOL and PL) muscle activity, using the equation:

$$\text{CCR} = \frac{\int \text{TA}}{\int \text{MG} + \int \text{SOL} + \int \text{PL}}$$

where each integration symbol represents the integrated EMG of the corresponding muscle. A ratio of 1 indicates pure co-contraction, whereas a ratio of 0 indicates no co-contraction from the tibialis anterior muscle.

Synchronization and timing considerations

Two separate computers were used for data collection in the present study. Kinematics, EMG and torque signals were recorded and synchronized in the first computer with Tracking Manager software (Qualisys AB) at a sampling rate of 1500 Hz for EMG and torque, and 150 Hz for kinematics. Ultrasound imaging and torque were recorded using a second computer with customized LabVIEW software (National Instruments) at a frame rate of 30 frames s^{-1}. A manual trigger was used to synchronize the signals recorded via both computers. In addition, to validate the synchronization, the torque was recorded in both computers.

Test–retest reliability and standard error of measurement (SEM)

The reliability for the variables used in the present study was tested on four healthy control subjects on two different days at least 1 week apart. Intraclass correlation coefficient (ICC) was calculated and ranged between 0.71 and 0.95 for all variables. The calculated SEM for each variable was: stiffness = 9.11 N mm^{-1}, EMD = 2.04 ms, pre-activation = 0.4 ms, H/M ratio = 0.02, V/M ratio = 0.1, CI = 0.04 and CCR = 0.08.

Statistical analysis

A paired sample t test was used to test the differences between the involved and non-involved limb in individuals with Achilles tendinosis for the seven parameters proposed in the present study. An independent sample t test was used to test the difference of side-to-side discordance between tendinotic and healthy control groups. Bonferroni correction was used to account for the multiple comparisons. The significance level after correction was set at $\alpha = 0.007$.

Results

Subjects demographics and anthropometrics

There was no difference between groups in age, body weight, body height and physical activity participation measured using GPAQ. There were significant differences between groups in VISA-A score and tendon thickness ($P = 0.04$ and $P < 0.001$, respectively) inherent to the study design. The difference in VISA-A score confirmed the history of Achilles tendinopathy. The average score on VISA-A for our tendinopathic subjects was 79.4/100 (Table 1). The Achilles tendon anterior–posterior thickness was higher on the involved side (involved: 7.6 ± 0.9 mm; uninvolved: 4.9 ± 0.6 mm; $P < 0.05$), which contributed to a larger side-to-side difference in tendinotic group. This side-to-side difference in tendon thickness was not observed in healthy subjects (right: 4.2 ± 0.5 mm; left: 4.4 ± 0.3 mm; $P > 0.05$). The difference in tendon thickness in tendinotic subjects confirmed the existence of Achilles tendinosis.

Tendon mechanical property

In the tendinotic group, the average stiffness was 295.39 ± 60.37 N mm^{-1} on the non-involved side and 164.82 ± 43.8 N mm^{-1} on the involved side, resulting in a side-to-side difference of 130.58 ± 37.97 N mm^{-1} ($44.08 \pm 9.12\%$). This difference was statistically significant ($P < 0.001$). In the healthy group, the average stiffness was 358.24 ± 33.43 N mm^{-1} on the right side and 360.47 ± 31.24 N mm^{-1} on the left side, resulting in a difference of 12.02 ± 7.36 N mm^{-1} ($3.34 \pm 2.14\%$). This difference was not statistically significant ($P = 0.637$) (Fig. 5A). When the between sides differences were compared between groups, the difference exceeded the SEM (9.11 N mm^{-1}) and was statistically different ($P < 0.001$).

EMD

In the tendinotic group, the average EMD was 29.44 ± 2.21 ms on the non-involved side and 39.44 ± 3.96 ms on the involved side, resulting in a side-to-side difference of 9.99 ± 3.16 ms ($34.11 \pm 11.65\%$). This difference was statistically significant ($P < 0.001$). In the healthy group, the average EMD was 38.21 ± 11.84 ms on the right side and 38.97 ± 11.83 ms on the left side, resulting in a difference of 1.68 ± 1.14 ms ($5.19 \pm 4.31\%$). This difference was not statistically significant ($P = 0.249$) (Fig. 5B). When the between sides differences were compared between groups, the difference exceeded the SEM (2.04 ms) and was statistically different ($P < 0.001$).
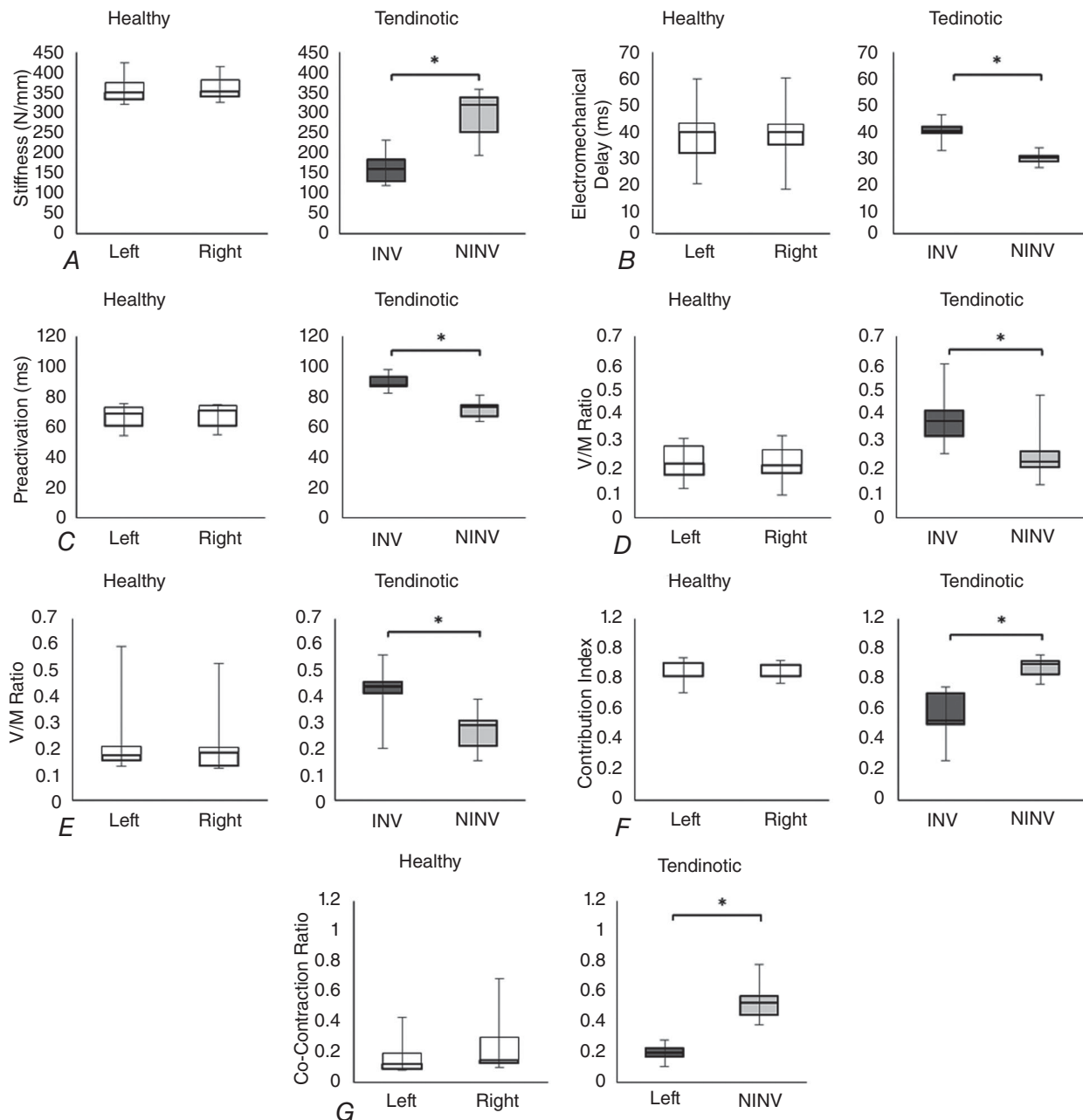
Preactivation

In the tendinotic group, the average preactivation was 71.64 ± 6.17 ms on the non-involved side and 90.01 ± 5.30 ms on the involved side, resulting in a side-to-side difference of 18.37 ± 6.58 ms ($26.27 \pm 10.54\%$). This difference was statistically significant ($P < 0.001$). In the healthy group, the average preactivation was 67.06 ± 7.43 ms on the right side and 67.82 ± 7.40 ms on the left side, resulting in a difference of 2.04 ± 1.25 ms ($2.98 \pm 1.86\%$). This difference was

not statistically significant ($P = 0.335$) (Fig. 5*C*). When the between sides differences were compared between groups, the difference exceeded the SEM (0.4 ms) and was statistically different ($P < 0.001$).

Central nervous system reponses

In the tendinotic group, the average *H/M* ratio was 0.24 ± 0.10 on the non-involved side and 0.38 ± 0.10 on the involved side, resulting in a side-to-side difference

Figure 5. Side-to-side comparison in individuals with and without Achilles tendinosis
A, stiffness. *B*, EMD. *C*, preactivation. *D*, *H/M* ratio. *E*, *V/M* ratio. *F*, CI. *G*, CCR. INV, involved; NINV, non-involved.

of 0.14 ± 0.04 ($66.91 \pm 35.37\%$). This difference was statistically significant ($P < 0.001$). In the healthy group, the average H/M ratio was 0.21 ± 0.07 on the right side and 0.21 ± 0.07 on the left side was, resulting in a difference of 0.02 ± 0.01 ($12.15 \pm 7.4\%$). This difference was not statistically significant ($P = 0.942$) (Fig. 5*D*). When the between sides differences were compared between groups, the difference exceeded the SEM (0.02) and was statistically different ($P < 0.001$).

In the tendinotic group, the average V/M ratio was 0.27 ± 0.08 on the non-involved side and 0.43 ± 0.10 on the involved side, resulting in a side-to-side difference of 0.16 ± 0.09 ($71.78 \pm 67.13\%$). This difference was statistically significant ($P = 0.001$). In the healthy group, the average V/M ratio was 0.21 ± 0.14 on the right side and 0.20 ± 0.12 on the left side, resulting in a difference of 0.02 ± 0.02 ($9.16 \pm 4\%$). This difference was not statistically significant ($P = 0.258$) (Fig. 5*E*). When the between sides differences were compared between groups, the difference exceeded the SEM (0.1) and was statistically different ($P < 0.001$).

CI

In the tendinotic group, the average CI was 0.88 ± 0.07 on the non-involved side and 0.57 ± 0.16 on the involved side, resulting in a side-to-side difference of 0.31 ± 0.11 ($36.19 \pm 15.07\%$). This difference was statistically significant ($P < 0.001$). In the healthy group, the average CI was 0.86 ± 0.08 on the right side and 0.86 ± 0.05 on the left side, resulting in a difference of 0.05 ± 0.05 ($5.9 \pm 5.49\%$). This difference was not statistically significant ($P = 0.91$) (Fig. 5*F*). When the between sides differences were compared between groups, the difference exceeded the SEM (0.04) and was statistically different ($P < 0.001$).

CCR

In the tendinotic group, the average CCR was 0.53 ± 0.12 on the non-involved side and 0.20 ± 0.05 on the involved side, resulting in a side-to-side difference of 0.32 ± 0.12 ($60.44 \pm 10.91\%$). This difference was statistically significant ($P < 0.001$). In the healthy group, the average CCR was 0.17 ± 0.12 on the right side and 0.25 ± 0.19 on the left side, resulting in a difference of 0.10 ± 0.11 ($34.98 \pm 19.69\%$). This difference was not statistically significant ($P = 0.09$) (Fig. 5*G*). When the between sides differences were compared between groups, the difference exceeded the SEM (0.08) and was statistically different ($P < 0.001$).

Table 2 shows the group means and average absolute individual side-to-side differences in tendinotic and healthy control subjects. After correction for multiple comparisons, a significant difference ($P < 0.007$) between the two groups was observed for all variables studied.

Discussion

The present study is the first to investigate the impact of a long standing musculoskeletal degenerative disorder on multi-level hierarchical system of human body. The reaffirming evidence reported in the present study indicates that tendinotic tendons are more compliant compared either to a healthy control group or to the contralateral side of the subjects themselves. This unilateral involvement affected the neuromuscular control on the involved side but not the non-involved side. The muscle–tendon unit on the tendinotic side exhibits a lowered temporal efficiency, which leads to altered CNS control. The altered CNS control is then expressed as an adapted muscle activation pattern in the lower leg.

The within subject design used in the present study provides a window into the adaptations as a consequence of a musculoskeletal disorder involving only one extremity. In all of the variables investigated in the present study, the side-to-side difference in healthy control subjects is significantly smaller than that in tendinotic subjects. Achilles tendinopathy may affect both legs but, when the -opathy presents as a focal mid-substance thickening in the region of 2–6 cm above the calcaneus signifying tendinosis, the thickening is seldom progressing at the same rate on both legs. The same difference in the rate of morphological changes would apply to non-overuse tendinoses, such as those related to hypercholesterolaemia or dyslipidaemia. Therefore, the invariance between sides in control and variance among tendinotic subjects suggests that these variables are capable of detecting pathology-induced side-to-side differences at tendon, muscle, muscle–tendon complex and CNS levels.

In the present study, the primary inclusion criterion for tendinotic group was a 2 mm difference in the anterior–posterior dimension between sides (tendinotic thicker than the non-tendinotic tendon). All tendinotic subjects recruited in the present study show fusiform focal thickening on ultrasound imaging, which is one of the most common abnormalities observed in clinical sonographic assessment of the Achilles tendon (Kälebo *et al.* 1992; Paavola *et al.* 1998). From clinical observations, the thickness change may take years to develop; therefore, this criterion ensures the chronicity of the tendon degeneration.

Despite the difference in tendon thickness between sides, the tendinotic subjects were pain-free when recruited and during the laboratory experiment. Pain is a signal of tissue damage, although damaged tissues are not always painful. In our cohort with Achilles tendinosis, diminished tendon properties were observed.

Table 2. Group means per side and average absolute individual side-to-side-differences for all tested variables

	Tendinotic (*n* = 9)			Healthy (*n* = 10)		
	Involved	Non-Involved	|Δ|	Right	Left	|Δ|
Stiffness (N mm^{-1})	164.82 ± 43.80*	295.39 ± 60.37	130.58 ± 37.97[†]	358.24 ± 33.43	360.47 ± 31.24	12.02 ± 7.36
EMD (ms)	39.44 ± 3.96*	29.44 ± 2.21	9.99 ± 3.16[†]	38.21 ± 11.84	38.97 ± 11.83	1.68 ± 1.14
Preactivation (ms)	90.01 ± 5.30*	71.64 ± 6.17	18.37 ± 6.58[†]	67.06 ± 7.43	67.82 ± 7.40	2.04 ± 1.25
H/*M* ratio	0.38 ± 0.10*	0.24 ± 0.10	0.14 ± 0.04[†]	0.21 ± 0.07	0.21 ± 0.07	0.02 ± 0.01
V/*M* ratio	0.43 ± 0.10*	0.27 ± 0.08	0.16 ± 0.09[†]	0.21 ± 0.14	0.2 ± 0.12	0.02 ± 0.02
CI	0.57 ± 0.16*	0.88 ± 0.07	0.31 ± 0.11[†]	0.86 ± 0.08	0.86 ± 0.05	0.05 ± 0.05
CCR	0.2 ± 0.05*	0.53 ± 0.12	0.32 ± 0.12[†]	0.17 ± 0.12	0.25 ± 0.19	0.10 ± 0.11

Data are presented as the mean ± SD. \|Δ\|: Average absolute individual side-to-side-differences in each group. *$P < 0.001$, when comparing the two sides within each group. †$P < 0.001$, when comparing the average absolute individual side-to-side-differences (\|Δ\|) between groups.

Although the individuals were not painful, they still yielded a lower VISA-A score compared to their healthy control counterpart. When compared with the healthy control subjects, the tendinotic subjects showed similar general physical activity level (GPAQ), even in the category of vigorous activity. These individuals might go back to their strenuous physical activities without alertness of the mechanical deficit accompanying tendinosis, which increases the risk of further injury to the tendinotic tendons (Gajhede-Knudsen *et al.* 2013). Clinically, symptoms such as pain and self-reported severity (VISA-A) have long been used as an indicator of recovery or the ability to return to sports activities (Silbernagel *et al.* 2011; Verrall *et al.* 2011). However, the mechanical characteristics of the tendon should also be taken into consideration to eliminate the risk of re-occurrence of symptoms or further injury such as tendon rupture.

The dissociation between tendon pain and tissue damage is commonly seen by clinicians. Abnormal changes on image modalities such as ultrasound can often be observed without tendon pain. Participants with tendinosis in the present study were recruited from clinics or referred by clinicians. All of the subjects in the tendinotic group experienced tendon pain in the past but not at the time of recruitment. The chronicity of their tendon degeneration, judging from the increased thickness, suggests that they are at the later stage on the tendon degeneration continuum.

To date, the research on the impact of Achilles tendon pain on neuromusculoskeletal function is limited. Pain of the Achilles tendon has been reported to lower electrical activities of the agonist, synergist and antagonist muscles (Henriksen *et al.* 2011). Because of the sporadic nature of the symptoms in Achilles tendinosis, it is critical to recruit subjects at the period when they are pain-free to capture the adaptations to the mechanical deficit accompanying Achilles tendinosis.

Mechanical properties of tendinotic Achilles

The results of the present study further confirm that the mechanical properties of the Achilles tendon are impacted in the presence of Achilles tendinosis. In individuals with Achilles tendinosis, the stiffness of the Achilles tendon is lower on the tendinotic side compared to the non-tendinotic side, as well as to healthy control subjects. The value of the stiffness of the non-tendinotic tendon in individuals with Achilles tendinosis and that of healthy control subjects is comparable with the stiffness values reported in the literature (Maganaris & Paul, 2002; Arya & Kulig, 2010). However, the stiffness of the tendinotic Achilles tendon is lower than the published data (120.93 ± 36.48 N mm^{-1} versus 300.37 ± 37.6 N mm^{-1}) (Arya & Kulig, 2010). The discrepancy may be the result of a more strict inclusion criteria (difference in tendon thickness >2 mm between sides) used in the present study. The stricter inclusion criteria emphasized a higher severity of morphological changes, hence further reducing the mechanical properties.

The average stiffness of the tendinotic Achilles tendons was 164.82 N mm^{-1}, which is at the lower end of the optimal range of tendon stiffness. Using computer simulation on human medial gastrocnemius muscle–tendon complex, (Lichtwark & Wilson (2008) determined that, to achieve optimal efficiency of this complex, the Achilles tendon has to perform in the range 150–500 N mm^{-1}. Computer simulation studies also reveal that muscle force generation can be affected by excessive tendon compliance (Ettema, 1996). Therefore, an optimal range of tendon stiffness is necessary for optimal tendon function. If optimal tendon function is not available, such as in the case of tendinosis, other components of the sensory–motor system will need to adapt. In the present case, this is seen with a higher contribution of other plantarflexors (peroneus longus), an enhanced feedforward mechanism (shorter preactivation)

and an enhanced gain of feedback control mechanism (higher H-reflex and V-wave).

The moment arm length of the Achilles tendon was estimated using the tendon excursion method (An *et al.* 1984; Maganaris & Paul, 2002). The use of this method is widely reported in the literature for estimating the tendon moment arm, and subsequently the tendon force, and it is considered to be a robust (Fath *et al.* 2010). However, the tendon excursion method underestimates the length of the Achilles tendon moment arm (by up to 30%) compared to the centre of rotation method utilizing magnetic resonance imaging (Fath *et al.* 2010). Thus, the force estimated using our approach may be higher than the actual force acting on the tendon.

Achilles tendon force was estimated by dividing the torque by moment arm length. The assumption for this estimation was that the torque as produced solely by the triceps surae muscle. Studied during cycling, the triceps surae accounts for ∼65% of ankle moment (Gregor *et al.* 1991). Therefore, the Achilles tendon force estimated in the present study may be higher than the actual force acting on the tendon.

The tendon stiffness is determined by the slope of the linear part of the force–elongation curve through the ramped isometric contraction. This method has been used to study the stiffness of the healthy and tendinotic Achilles tendons in the literature (Maganaris & Paul, 2002; Arya & Kulig, 2010). With this approach, the potential error from estimating stiffness using only one data point at the MVIC can be eliminated, and the data yield high reliability.

Tendon elongation was measured in the present study by using the combination of ultrasound scanning and motion capture. Using ultrasound alone to measure the tendon elongation by tracking the fascicle displacement has been criticized and invalidated as a result of (1) displacement of ultrasound transducer on the skin and (2) rotation (dorsiflexion) of the calcaneus during movement (Maganaris, 2005). Adding the use of motion capture in the present study allowed us to quantify and account for these displacements, making the tendon elongation measurement more viable and valid.

Taken together, two assumptions, tendon moment arm estimated by tendon excursion method and ankle torque produced solely by the triceps surae muscle, were made to measure tendon mechanical properties, as discussed above. Both assumptions lead to an over-estimation of the tendon force. These assumptions were inevitable in non-invasive, *in vivo* human subject experiments. Such an over-estimation, however, does not affect the difference between sides in tendon mechanical properties in tendinotic subjects observed in the present study.

As a point of interest, we do not report, or discuss, the material properties (elastic modulus) of the tendons. Modulus is a normalized measure of stiffness and all the tendinotic tendons included in the present study had significant focal thickening, making the comparison rather driven by the tendon morphology and not the mechanical properties.

Temporal efficiency of the triceps surae musculotendinous unit in the presence of Achilles tendinosis

The EMD is a response to current mechanical properties of the musculotendinous unit; therefore, it responds to diminished load and to exercise training. The EMD for the involved side in tendinotic subjects was longer (39.44 ± 3.96 ms) than that on the non-involved side (29.44 ± 2.21 ms). This difference was statistically significant and physiologically hypothesized as an adaptation to a more complaint tendon. The EMDs for the healthy controls have mean values similar to those of the tendinotic (involved) side; however, the SDs are higher in the control group (11.84 ms and 11.83 ms) than in the tendinotic group (3.96 ms and 2.21 ms). This wider range of EMD data in the control group encompasses the range represented by the tendinotic group. The data in both groups represent the data found in the literature reporting electrically-induced EMD for plantar flexors between 15 and 50 ms (Muraoka *et al.* 2004; Esposito *et al.* 2011).

The EMD has been reported to correlate with tendon stiffness in healthy tendons, as well as in pathological tendons with no well defined morphology (Kubo *et al.* 2001; Muraoka *et al.* 2004; Wang *et al.* 2012). Our data represent strong evidence indicating that, in the presence of tendon degeneration, the triceps surae musculotendinous unit functions under a compromised temporal efficiency.

Spinal and supraspinal plasticity in Achilles tendinosis

Individuals with Achilles tendinosis showed an up-regulated spinal reflex at rest (H-reflex) and a supraspinal response during maximal voluntary contraction (V-wave) on the involved side compared to the non-involved side, as well as to that of healthy control subjects. The H-reflex and V-wave are indicators of CNS excitability, where the H-reflex represents the motor neuron excitability and the V-wave includes the contribution from supraspinal centres.

An enhanced resting H-reflex was observed on the tendinotic limb in individuals with Achilles tendinosis, suggesting elevated α-motoneuron excitability. This increased α-motoneuron excitability may be attributed to suppressed presynaptic inhibition compensating for the slackness of the muscle–tendon unit. However, this is different from the consequence of passive muscle stretching. When stretching, the muscle spindle is stretched, which enhances the presynaptic inhibition and, consequently, the suppressed H-reflex response (Robertson *et al.* 2012).

An elevated V-wave was also seen on the tendinotic limb in individuals with Achilles tendinosis in the present study, which indicates an up-regulated descending neural drive. As noted earlier, the development of Achilles tendinosis is a prolonged process, which usually takes years to develop significant changes in tendon morphology. This prolonged process enabled the CNS to adapt to the altered mechanical characteristics of the tendon. Because the muscle spindle activity and α-motoneuron excitability may be elevated to compensate for the diminished Ib afferent input, the motor cortex excitability is up-regulated in the form of an increased V-wave, over a prolonged period of time. This enhancement of the V-wave is similar to that observed in strength training (Voigt *et al.* 1998; Aagaard *et al.* 2002; Gondin *et al.* 2006; Fimland *et al.* 2009).

In the present study, both the H-reflex and the V-wave were higher on the side of Achilles tendinosis, suggesting that the modulations are attributed not only to the supra-spinal centres, but also to the neural mechanisms at the spinal level. In a similar study by Wang *et al.* (2011) conducted in a much younger cohort, the V-wave was elevated on the tendinopathic side, yet the H-reflex was not. The cortical adaptations seen in both studies may persist in later stages of the disease, as seen in our older cohort. It is not clear, however, whether the spinal adaptations are initiated at the early stage of tendinopathy or are more prominent later because the present study showed changes in the H-reflex, which was not observed in the study by Wang *et al.* (2011).

The H-reflex and V-wave are sensitive CNS responses that may be affected by multiple complex mechanisms (Misiaszek, 2003; Knikou, 2008). Therefore, the CNS responses investigated in the present study are the first step in exploring the CNS adaptations to the mechanical deficit accompanying a musculoskeletal disorder. To understand the underlying mechanisms or to pin-point the location of these adaptations, it might be pertinent to resort to other neural probes such as transcranial magnetic stimulation or functional magnetic resonance imaging in future studies. With transcranial magnetic stimulation, researchers are able to observe the effect of exercise training on spinal versus intracortical excitability, with a reduced inhibitory mechanism being reported within the M1 area after training (Weier *et al.* 2012). Using the same technique, mechanisms of the corticospinal adaptations to Achilles tendinosis can be explored further.

Altered preactivation during hopping in the presence of Achilles tendinosis

During hopping, individuals with Achilles tendinosis exhibit an earlier preactivation of the medial gastro-cnemius muscle on the involved side. The preactivation of the triceps surae muscle comprises a centrally programmed feedforward control (Funase *et al.* 2001;

Hobara *et al.* 2007). As a result of the nature of pre-programmed feedforward control, preactivation is independent of the rate of hopping (Funase *et al.* 2001) and also independent of the height of drop landing (Santello & McDonagh, 1998). Therefore, preactivation properly adjusts the position and stiffness of the ankle joint at landing (Müller *et al.* 2012). The present study demonstrated that the timing of medial gastrocnemius muscle activation was earlier in individuals with Achilles tendinosis, aiming to compensate for the diminished temporal efficiency accompanying tendinosis and to achieve an appropriate ankle joint angle and stiffness for landing.

Altered CNS motor control in the presence of Achilles tendinosis

Based on the internal model of human motor control, the control mechanism relies on two pathways to control the body to achieve a desired position: feedforward and feedback (Kawato, 1999). During rhythmic bipedal or unipedal movements, feedback provides information from the interaction with the environment. This information enables the control system to adjust to the current (online regulatory feedback) or next (adaptive feedback) movement. Feedforward, however, utilizes the information learned from past experience to control the body parts to reach a desired position, which allows the body to reach the desired position faster (Desmurget & Grafton, 2000).

In individuals with Achilles tendinosis, as a result of impaired Ib afferent input accompanying a compliant tendon, the timing of the feedback control is compromised, which means that the delay in the feedback loop is prolonged. Therefore, feedback control cannot provide prompt online regulatory information to reach the desired body position. To compensate for this deficiency, the gain of the feedback control increases in the form of an up-regulated H-reflex and V-wave as discussed above (Kawato, 1999).

The control system, with delayed but enhanced feedback control, may rely more on the feedforward control. However, the reduced temporal efficiency of the musculotendinous unit also impacts upon the execution of feedforward control, which makes the adaptation of the feedforward control necessary. The alteration in feedforward control is manifested as earlier preactivation during hopping in the present study.

Effect of Achilles tendinosis on the agonist, synergist and antagonist muscles

In addition to the altered control system, the present study also observed an adaptive behaviour, as illustrated by the activity of agonist, synergist and antagonist muscles.

This was seen during single-legged hopping, where the contribution from the triceps surae muscle to the plantar flexors was decreased and the co-contraction from the tibialis anterior muscle was also decreased on the involved side in individuals with Achilles tendinosis. This may be attributed to the protective mechanism shielding the already injured tendon from further injury or even rupture (Lund *et al.* 1991). Meanwhile, the lowered contribution to plantar flexion from the triceps surae muscle was compensated for by other plantar flexors, such as the peroneal longus in the present study. The protective mechanism may also impact the antagonists (i.e. tibialis anterior). During hopping, the co-contraction from the tibialis anterior decreased, suggesting less antagonist muscle activity and hence less stress on the Achilles tendon.

Experience of pain may be the origin of the protective mechanism described above. Although pain-free at the time of participation, the tendinotic subjects in the present study experienced tendon pain in the past. In a study on experimental Achilles tendon pain induced by intra-tendinous saline injection in healthy subjects, Henriksen *et al.* (2011) reported an immediate reduction in EMG activity in agonist, synergist and antagonist muscles. The reduction in EMG activity as a result of pain probably persists in individuals with Achilles tendinosis, even when the pain has subsided. Furthermore, the EMG activity of the synergist muscle, the peroneal longus muscle in the present study, increased to compensate for the mechanical deficit resulting from the compliant Achilles tendon and to achieve the task goal. This phenomenon of increased activity of synergistic muscles has been modelled and reported in the fingers (Valero-Cuevas, 2005).

It is important to discuss our tendinotic subjects' bilateral CCR data with respect to the data of control subjects. The CCR data presented with similar within-group and between-group relationships as seen with the EMD, such that the involved side of the tendinotic group had less (0.2 ± 0.05) co-contraction than the non-involved side (0.53 ± 0.12). That difference was statistically significant and physiologically hypothesized as a consequence of motor control adaptations aimed at decreasing the demand on the plantar flexors by minimizing the activity of the dorsi-flexor during unipedal hopping. The CCR was similar between legs in the control group ($0.17 + 0.12$ for the right leg and $0.25 + 0.19$ for the left leg). Furthermore, when compared with the tendinotic group, the means were similar to those of the involved side (0.2 ± 0.05).

Taken as a single unique variable, we do not have a grounded explanation for this between-group comparison, although we attribute this to the convenience sample in the present study and a wide range of values for CCR in all of the subjects studied (0.1–0.8). Because we were unable to identify a study reporting on CCR during hopping, we encourage the scientific community to explore this variable further.

Limitations and suggestions

One of the limitations of the present study is the direct generalizability of our findings. Because our inclusion criteria narrowed the cohort of participants to advanced morphologically-confirmed tendinopathy (i.e. tendinosis), the measured adaptations apply to tendinosis only and not a broad range of tendinopathies including an -itis. It would certainly be very meaningful to explore the time-course of these multi-level adaptations by studying earlier stages of tendinopathy. Studies should also explore further whether any, or all, of these adaptations are reversible to the pre-degenerative status by a well-reasoned intervention. Although all involved Achilles tendons were thicker than those on the contralateral side, we are unable to conclude whether the histopathology of the non-involved side has shown any signs of hypercellularity or vascular proliferation that is suggestive of central neuronal adaptations to unilateral tendinosis observed in a rabbit model by Andersson *et al.* (2011).

The present study also carries inherent limitations of an *in vivo* human subject experiment. We incorporated the participant's volition during isometric ramped contraction when determining force–elongation curves and adding the volitional contraction to electrically elicited measures of reflexive activation (V-wave). To determine preactivation and co-activation, we required the participants to hop in place to the beat of a metronome. Those types of factors, in addition to the need for positioning of the subjects in the testing apparatus in a specific and predetermined way, make the investigator rely on extensive preliminary work in the laboratory and also controlled repeated-measure experiments preceding the main experiment. Those repeated separate day measures on the same subjects allow not only determination of variation in the data but also the calculation of the SEM that provides for an error-related comparison between sides and groups, in addition to the traditional reliance of statistics.

Taken together, the results obtained in the present study illustrate the co-ordinated multi-level adaptations to a mechanical lesion in a human tendon caused by pathology. These types of adaptations to tissue degeneration are physiologically expected but not always observable.

References

Aagaard P, Simonsen EB, Andersen JL, Magnusson P & Dyhre-Poulsen P (2002). Neural adaptation to resistance training: changes in evoked V-wave and H-reflex responses. *J Appl Physiol* **92**, 2309–2318.

An KN, Takahashi K, Harrigan TP & Chao EY (1984). Determination of muscle orientations and moment arms. *J Biomech Eng* **106**, 280–282.

Andersson G, Forsgren S, Scott A, Gaida JE, Stjernfeldt JE, Lorentzon R, Alfredson H, Backman C & Danielson P (2011). Tenocyte hypercellularity and vascular proliferation in a rabbit model of tendinopathy: contralateral effects suggest the involvement of central neuronal mechanisms. *Br J Sports Med* **45**, 399–406.

Armstrong T & Bull F (2006). Development of the world health organization global physical activity questionnaire (GPAQ). *J Public Health* **14**, 66–70.

Arya S & Kulig K (2010). Tendinopathy alters mechanical and material properties of the Achilles tendon. *J Appl Physiol* **108**, 670–675.

Cavanagh PR & Komi PV (1979). Electromechanical delay in human skeletal muscle under concentric and eccentric contractions. *Eur J Appl Physiol Occup Physiol* **42**, 159–163.

Child S, Bryant AL, Clark RA & Crossley KM (2010). Mechanical properties of the achilles tendon aponeurosis are altered in athletes with achilles tendinopathy. *Am J Sports Med* **38**, 1885–1893.

Desmurget M & Grafton S (2000). Forward modeling allows feedback control for fast reaching movements. *Trends Cogn Sci* **4**, 423–431.

Duclay J & Martin A (2005). Evoked H-reflex and V-wave responses during maximal isometric, concentric, and eccentric muscle contraction. *Journal of neurophysiology* **94**, 3555–3562.

Esposito F, Limonta E & Cè E (2011). Passive stretching effects on electromechanical delay and time course of recovery in human skeletal muscle: new insights from an electromyographic and mechanomyographic combined approach. *Eur J Appl Physiol* **111**, 485–495.

Ettema GJ (1996). Mechanical efficiency and efficiency of storage and release of series elastic energy in skeletal muscle during stretch-shorten cycles. *J Exp Biol* **199**, 1983–1997.

Fath F, Blazevich AJ, Waugh CM, Miller SC & Korff T (2010). Direct comparison of in vivo Achilles tendon moment arms obtained from ultrasound and MR scans. *J Appl Physiol (1985)* **109**, 1644–1652.

Fimland MS, Helgerud J, Gruber M, Leivseth G & Hoff J (2009). Functional maximal strength training induces neural transfer to single-joint tasks. *Eur J Appl Physiol* **107**, 21–29.

Funase K, Higashi T, Sakakibara A, Imanaka K, Nishihira Y & Miles TS (2001). Patterns of muscle activation in human hopping. *Eur J Appl Physiol* **84**, 503–509.

Gajhede-Knudsen M, Ekstrand J, Magnusson H & Maffulli N (2013). Recurrence of Achilles tendon injuries in elite male football players is more common after early return to play: an 11-year follow-up of the UEFA Champions League injury study. *Br J Sports Med* **47**, 763–768.

Gardiner P, Michel R, Browman C & Noble E (1986). Increased EMG of rat plantaris during locomotion following surgical removal of its synergists. *Brain Res* **380**, 114–121.

Gondin J, Duclay J & Martin A (2006). Soleus-and gastrocnemii-evoked V-wave responses increase after neuromuscular electrical stimulation training. *J Neurophysiol* **95**, 3328–3335.

Gregor RJ, Komi PV, Browning RC & Järvinen M (1991). A comparison of the triceps surae and residual muscle moments at the ankle during cycling. *J Biomech* **24**, 287–297.

Grosset JF, Piscione J, Lambertz D & Perot C (2009). Paired changes in electromechanical delay and musculo-tendinous stiffness after endurance or plyometric training. *European journal of applied physiology* **105**, 131–139.

Henriksen M, Aaboe J, Graven-Nielsen T, Bliddal H & Langberg H (2011). Motor responses to experimental Achilles tendon pain. *Br J Sports Med* **45**, 393–398.

Hobara H, Kanosue K & Suzuki S (2007). Changes in muscle activity with increase in leg stiffness during hopping. *Neurosci Lett* **418**, 55–59.

Kälebo P, Allenmark C, Peterson L & Swärd L (1992). Diagnostic value of ultrasonography in partial ruptures of the Achilles tendon. *Am J Sports Med* **20**, 378–381.

Kawato M (1999). Internal models for motor control and trajectory planning. *Curr Opin Neurobio* **9**, 718–727.

Knikou M (2008). The H-reflex as a probe: pathways and pitfalls. *J Neurosci Meth* **171**, 1–12.

Kongsgaard M, Qvortrup K, Larsen J, Aagaard P, Doessing S, Hansen P, Kjaer M & Magnusson SP (2010). Fibril morphology and tendon mechanical properties in patellar tendinopathy: effects of heavy slow resistance training. *Am J Sports Med* **38**, 749–756.

Kubo K, Kanehisa H & Fukunaga T (2002). Effects of resistance and stretching training programmes on the viscoelastic properties of human tendon structures in vivo. *J Physiol* **538**, 219–226.

Kubo K, Kanehisa H, Ito M & Fukunaga T (2001). Effects of isometric training on the elasticity of human tendon structures in vivo. *J Appl Physiol* **91**, 26–32.

Lichtwark GA & Wilson AM (2008). Optimal muscle fascicle length and tendon stiffness for maximising gastrocnemius efficiency during human walking and running. *J Theor Biol* **252**, 662–673.

Loeb G, Brown I & Cheng E (1999). A hierarchical foundation for models of sensorimotor control. *Exp Brain Res* **126**, 1–18.

Lund JP, Donga R, Widmer CG & Stohler CS (1991). The pain-adaptation model: a discussion of the relationship between chronic musculoskeletal pain and motor activity. *Can J Physiol Pharmacol* **69**, 683–694.

Maganaris CN (2005). Validity of procedures involved in ultrasound-based measurement of human plantarflexor tendon elongation on contraction. *J Biomech* **38**, 9–13.

Maganaris CN & Paul JP (2002). Tensile properties of the in vivo human gastrocnemius tendon. *J Biomech* **35**, 1639–1646.

Misiaszek JE (2003). The H-reflex as a tool in neurophysiology: its limitations and uses in understanding nervous system function. *Muscle Nerve* **28**, 144–160.

Müller R, Siebert T, Blickhan R, Müller R, Siebert T & Blickhan R (2012). Muscle preactivation control: simulation of ankle joint adjustments at touch down during running on uneven ground. *J Appl Biomech* **28**, 718–25.

Muraoka T, Muramatsu T, Fukunaga T & Kanehisa H (2004). Influence of tendon slack on electromechanical delay in the human medial gastrocnemius in vivo. *J Appl Physiol* **96**, 540–544.

Paavola M, Paakkala T, Kannus P & Jarvinen M (1998). Ultrasonography in the differential diagnosis of Achilles tendon injuries and related disorders. A comparison between pre-operative ultrasonography and surgical findings. *Acta Radiol* **39**, 612–619.

Robertson CT, Kitano K, Koceja DM & Riley ZA (2012). Temporal depression of the soleus H-reflex during passive stretch. *Exp Brain Res* **219**, 217–225.

Robinson J, Cook JL, Purdam C, Visentini P, Ross J, Maffulli N, Taunton J & Khan K (2001). The VISA-A questionnaire: a valid and reliable index of the clinical severity of Achilles tendinopathy. *Br J Sports Med* **35**, 335–341.

Santello M & McDonagh M (1998). The control of timing and amplitude of EMG activity in landing movements in humans. *Exp Physiol* **83**, 857–874.

Scott SH (2004). Optimal feedback control and the neural basis of volitional motor control. *Nat Rev Neurosci* **5**, 532–546.

Silbernagel KG, Brorsson A & Lundberg M (2011). The majority of patients with Achilles tendinopathy recover fully when treated with exercise alone: a 5-year follow-up. *Am J Sports Med* **39**, 607–613.

Upton AR, McComas AJ & Sica RE (1971). Potentiation of "late" responses evoked in muscles during effort. *Journal of neurology, neurosurgery, and psychiatry* **34**, 699–711.

Valero-Cuevas FJ (2005). An integrative approach to the biomechanical function and neuromuscular control of the fingers. *J Biomech* **38**, 673–684.

Verrall G, Schofield S & Brustad T (2011). Chronic Achilles tendinopathy treated with eccentric stretching program. *Foot Ankle Int* **32**, 843–849.

Voigt M, Chelli F & Frigo C (1998). Changes in the excitability of soleus muscle short latency stretch reflexes during human hopping after 4 weeks of hopping training. *Eur J Appl Physiol Occup Physiol* **78**, 522–532.

Wang HK, Lin KH, Su SC, Shih TF & Huang YC (2012). Effects of tendon viscoelasticity in Achilles tendinosis on explosive performance and clinical severity in athletes. *Scand J Med Sci Sports* **22**, e147–e155.

Wang HK, Lin KH, Wu YK, Chi SC, Shih TT & Huang YC (2011). Evoked spinal reflexes and force development in elite athletes with middle-portion Achilles tendinopathy. *J Orthop Sports Phys Ther* **41**, 785–794.

Wang JH (2006). Mechanobiology of tendon. *J Biomech* **39**, 1563–1582.

Weier AT, Pearce AJ & Kidgell DJ (2012). Strength training reduces intracortical inhibition. *Acta Physiol* **206**, 109–119.

Wolpert DM, Pearson KG & Ghez CPJ (2013). The organization and planning of movement. In *Principles of Neural Science, 5 edn*, ed. Kandel ER, Schwartz JH, Jessell TM, Siegelbaum SA & Hudspeth AJ, pp. 743–766. McGraw-Hill, New York, NY.

Additional information

Competing interests

The authors declare that they have no competing interests.

Author contributions

Y-JC and KK contributed to the conception and design of the experiments, analysis and interpretation of data, and drafting and revision of the article. Y-JC collected the data.

Funding